molecules

MDPI

Article

Furan-Indole-Chromenone-Based Organic Photocatalyst for α-Arylation of Enol Acetate and Free Radical Polymerization Under LED Irradiation

Aurélien Galibert-Guijarro [1], Adel Noon [2,3,4], Joumana Toufaily [4], Tayssir Hamieh [2,4,5], Eric Besson [1], Stéphane Gastaldi [1], Jacques Lalevée [2,3,*] and Laurence Feray [1,*]

1 Aix Marseille Univ, CNRS, ICR, 13013 Marseille, France; aurelien.galibert@univ-amu.fr (A.G.-G.); eric.besson@univ-amu.fr (E.B.); stephane.gastaldi@univ-amu.fr (S.G.)
2 Université de Haute-Alsace, CNRS, IS2M UMR 7361, F-68100 Mulhouse, France; adelnoon@gmail.com (A.N.); t.hamieh@maastrichtuniversity.nl (T.H.)
3 Université de Strasbourg, F-67000 Strasbourg, France
4 Laboratory of Materials, Catalysis, Environment and Analytical Methods (MCEMA), Faculty of Sciences, Doctoral School of Sciences and Technology (EDST), Lebanese University, Beirut 6573-14, Lebanon; joumana.toufaily@ul.edu.lb
5 Faculty of Science and Engineering, Maastricht University, P.O. Box 616, 6200 MD Maastricht, The Netherlands
* Correspondence: jacques.lalevee@uha.fr (J.L.); laurence.feray@univ-amu.fr (L.F.)

Abstract: In this study we report on the efficiency of a furane-indole-chromenone-based organic derivative (**FIC**) as a photocatalyst in the α-arylation of enol acetate upon LED irradiation at 405 nm, and as a photoinitiator/photocatalyst in the free radical polymerization of an acrylate group in the presence of *bis*-(4-*tert*-butylphenyl)iodonium hexafluorophosphate (Iod) as an additive, or in the presence of both Iod and ethyl-4-(dimethyl amino) benzoate (EDB) under LED irradiation at 365 nm. The photochemical properties of this new light-sensitive compound are described, and the wide redox window (3.27 eV) and the high excited-state potentials **FIC***/**FIC**$^{\bullet-}$ (+2.64 V vs. SCE) and **FIC**$^{\bullet+}$/**FIC*** (−2.41 V vs. SCE) offered by this photocatalyst are revealed. The chemical mechanisms that govern the radical chemistry are discussed by means of different techniques, including fluorescence-quenching experiments, UV-visible absorption and fluorescence spectroscopy, and cyclic voltammetry analysis.

Keywords: organic photocatalyst; free radical polymerization; alkene arylation; photoredox catalysis; redox potential; photoinduced electron transfer

check for updates

Academic Editor: Shunichi Fukuzumi

Received: 21 November 2024
Revised: 6 January 2025
Accepted: 9 January 2025
Published: 11 January 2025

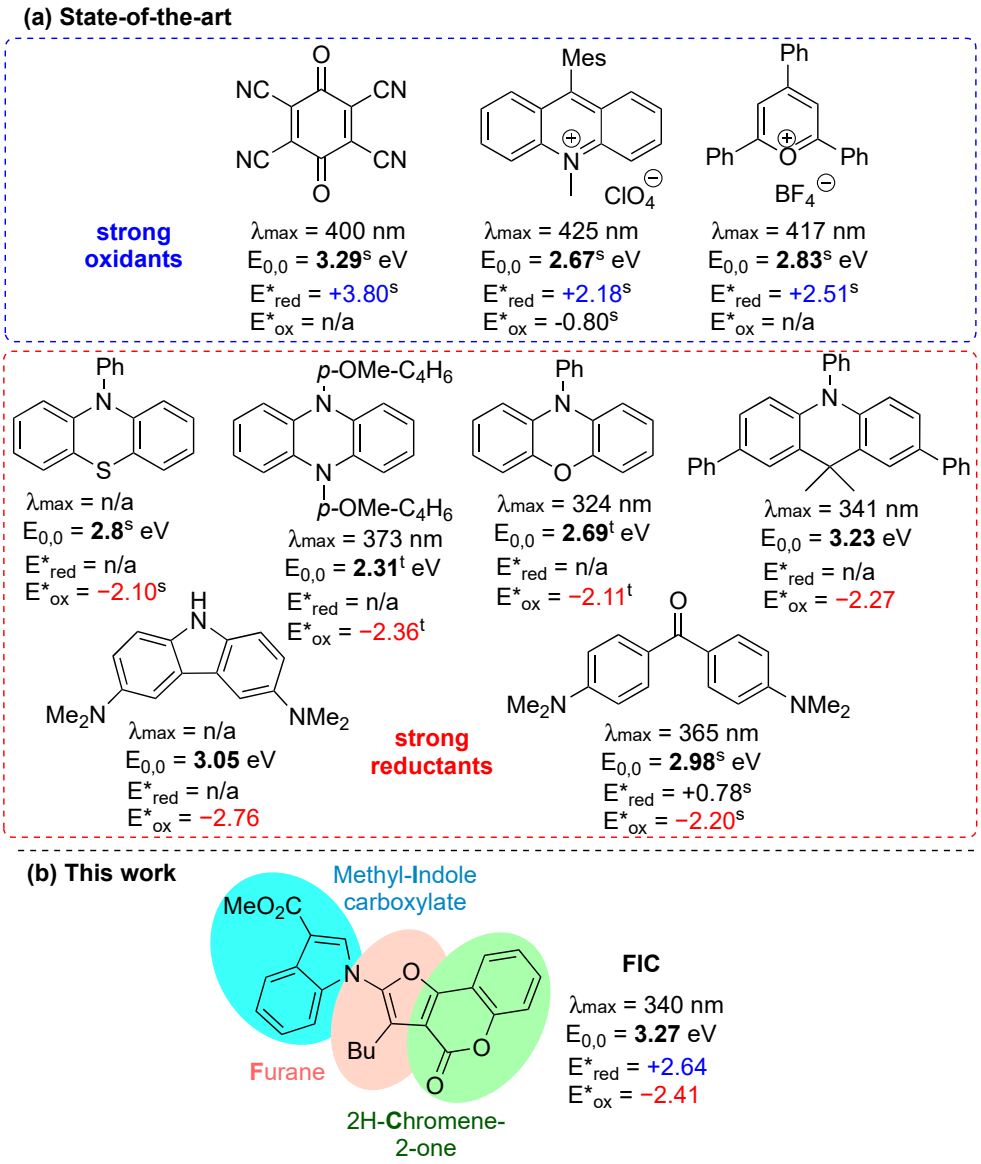
Citation: Galibert-Guijarro, A.; Noon, A.; Toufaily, J.; Hamieh, T.; Besson, E.; Gastaldi, S.; Lalevée, J.; Feray, L. Furan-Indole-Chromenone-Based Organic Photocatalyst for α-Arylation of Enol Acetate and Free Radical Polymerization Under LED Irradiation. *Molecules* **2025**, *30*, 265. https://doi.org/10.3390/molecules30020265

Copyright: © 2025 by the authors. Licensee MDPI, Basel, Switzerland. This article is an open access article distributed under the terms and conditions of the Creative Commons Attribution (CC BY) license (https://creativecommons.org/licenses/by/4.0/).

1. Introduction

Over the past decade, photochemical transformations have received increasing attention. In particular, photocatalyzed reactions using visible light as a photon source are now recognized as an essential and useful organic synthesis platform to access a wide range of complex molecular structures. In most visible-light photocatalyzed reactions, the activation mode involves a photocatalyst in its excited state being able to donate or take an electron from a substrate to form radical species [1,2]. Until recently, ruthenium- and iridium-based photocatalysts were the most representative in this field, but the need to find catalysts free of rare or toxic metals led organic chemists to take a closer look at photosensitive organic molecules, which present advantages in terms of cost and availability [3,4]. However, in relation to this field of research, there are still opportunities for further exploration, such as the development of more robust chromophores with highly reducing and/or oxidizing

potentials (Scheme 1a) [5,6]. Thus, tuning the properties of already known architectures to increase their photocatalytic efficiencies, as well as to discover new photosensitive molecules, has become a challenging field of research [7,8].

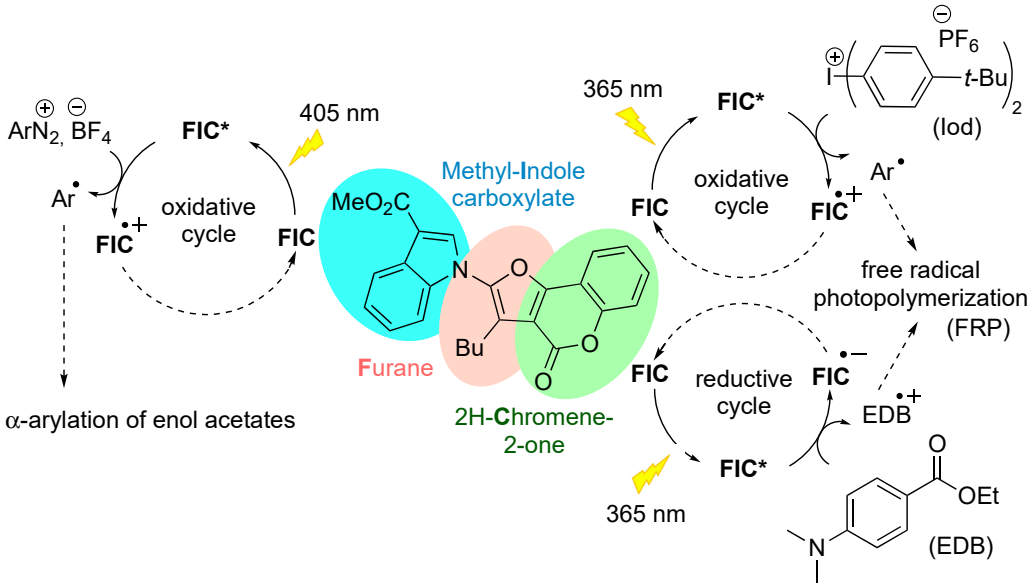


Scheme 1. Organic photocatalysts (PCs) with high excited-state reduction and/or oxidation potentials E^*_{red} ($PC^*/PC^{\bullet-}$) > +2 V and/or E^*_{ox} ($PC^{\bullet+}/PC^*$) < −2 V vs. SCE. n/a: Data not available. ^{s}: data for singlet excited state. ^{t}: data for triplet excited state. Reported excited-state redox potentials E* V vs. SCE, see ref. [6].

Photosensitive organic molecules can also find applications in polymer chemistry [9,10]. Indeed, photopolymerization technologies have prevailed recently, increasing focus over other conventional industrial processes that offer low energy consumption and excellent time and spatial control without the use of volatile organic compounds [11,12]. This allows them to be widely implemented in many fields, including adhesives, coatings, 3D printing, dental materials, microelectronics, etc. [13–15]. The latest advancements in this context include the development of photoinitiating systems that employ visible light-emitting diodes (LEDs) as alternative irradiation sources to the traditional UV mercury lamps. The advantages offered by the former are low power consumption, low heat generation, low operating costs, longer emission wavelengths (and therefore more in-dept

curing), safety, simplicity, portability, and easy availability [16,17]. Enormous effort has been dedicated to the development of new, highly efficient organic light sensitive molecules for applications both in organic synthesis and photopolymerizations.

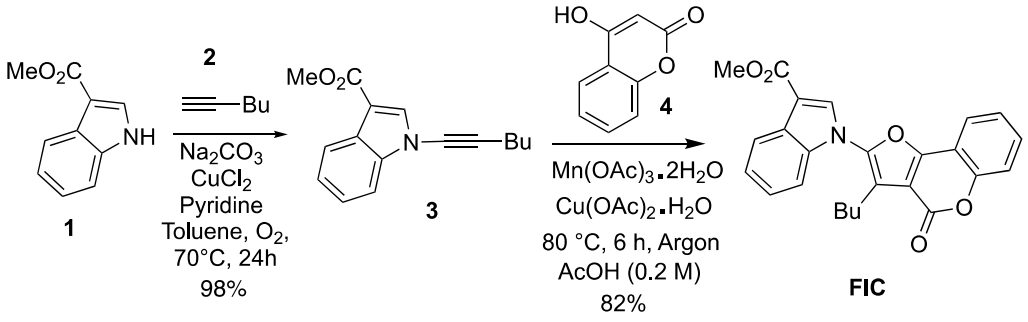
During the course of our investigation on the reactivity of ynamides towards radical transformations, we have synthesized a persubstituted furane bearing methyl-indole carboxylate and 2H-chromene-2-one units [18], which we called **FIC** (Scheme 1b). As this compound contained aromatic rings and various groups or heteroatoms with acceptor and donor effects, we decided to investigate its behavior in photocatalyzed reactions, in particular its ability to promote the formation of aryl radicals from aryldiazonium and aryliodonium salts using an oxidative cycle. Thus, in this study, we report on the efficiency of **FIC** as a photocatalyst in the α-arylation of enol acetate under LED irradiation at 405 nm, and as a photoinitiating system in the free radical polymerization of an acrylate derivative in the presence of *bis*-(4-*tert*-butylphenyl)iodonium hexafluorophosphate (Iod) as an additive or in the presence of both Iod and ethyl-4-(dimethyl amino) benzoate (EDB) under LED irradiation (@365 nm) (Scheme 2). The chemical mechanisms governing the interaction between **FIC** with both additives (Iod and EDB) to produce initiating radicals have been fully detailed by performing fluorescence quenching experiments, combining UV-visible absorption and fluorescence spectroscopy, and cyclic voltammetry analysis.



Scheme 2. α-Arylation of enol acetate and free radical polymerization of acrylate group mediated by **FIC**.

2. Results and Discussion

The synthesis of **FIC** can be achieved in two steps involving (i) cross-coupling reaction between commercially available 3-methyl indole carboxylate **1** and hex-1-yne **2** to give ynamide **3**, followed by (ii) Mn(III)/Cu(II)-mediated radical reaction of the latter with 4-hydroxycoumarine **4** leading to the desired compound (**FIC**) in an overall yield of 80% (Scheme 3) [18].

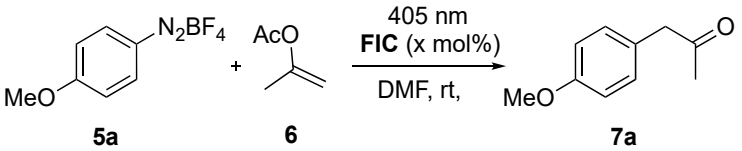


Scheme 3. Two-step synthesis of **FIC**.

2.1. α-Arylation of Enol Acetate

Aryl diazonium salts are versatile building blocks in organic chemistry that can be used as powerful aryl radical precursors under various conditions [19,20]. Light-mediated arylation of alkenes, alkynes, enones [21], or enol acetates [22] has been achieved with diazonium salts in the presence of several metal- or organic-based photocatalysts, and can be considered as a reference reaction for the evaluation of a new photocatalyst.

Arylation of isopropenyl acetate **6** with *p*-methoxybenzenediazonium tetrafluoroborate **5a** bearing a methoxy group was chosen as a model reaction to bring the first proof of concept (Scheme 4, Table 1). In the absence of **FIC**, after 2 h of irradiation at 405 nm in DMF, the solvent of choice to favor monoelectronic transfer [19], the reaction of diazonium salt **5a** with 10 equiv of enol acetate **6** led to a mixture of arylated expected ketone **7a**, and starting diazonium salt **5a** in a 20:80 ratio determined by ^{1}H NMR carried out on the crude reaction mixture (Table 1, entry 1). The presence of 10 mol% of **FIC** clearly reversed the ratio in favor of **7a** (Table 1, entry 2). It should be noted that repeating the reaction in the dark led to no significant conversion, which emphasizes the importance of light in this process. Similar results were observed when the reaction was conducted in air or in the presence of one equivalent of TEMPO. Reactions involving **FIC** were also conducted in DMSO, leading to poor conversions of **5a** compared to those obtained in DMF. Optimized conditions, i.e., the use of 15 equiv of enol acetate in DMF, enabled the reaction to be completed in 4 h, leading to the formation of **7a** isolated in a yield of 80% after purification (Table 1, entry 4). Under the same conditions, without the photocatalyst, the diazonium salt was partially consumed and compound **7a** was isolated in a yield of 30% (Table 1, entry 3), showing the crucial role of **FIC** in this light-driven process.



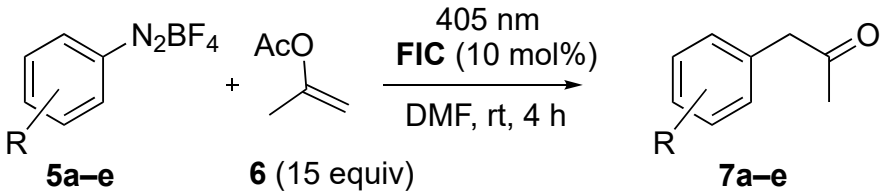
Scheme 4. Arylation of enol acetate **6** with diazonium salt **5a**.

Table 1. Initial investigation: arylation of enol acetate **6** with diazonium salt **5a**.

Entry	6 (Equiv)	t (h)	FIC (mol%)	7a:5a [1]	7a (%) [2]
1	10	2	-	20:80	nd [3]
2	10	2	10	70:30 [4]	nd [3]
3	15	4	-	-	30
4	15	4	10	-	80 [5]

[1] ^{1}H NMR ratio determined on the crude reaction mixture. [2] Isolated yield. [3] nd: not determined. [4] No conversion in ketone **7a** was observed when the reaction was conducted in the dark—in air—or in the presence of TEMPO (1 equiv). [5] A similar experiment was reported with Ru(II) as the photocatalyst to give a yield of 40% for **7a** (see ref. [22]).

The scope of the transformation was studied by reacting enol acetate **6** with different diazonium tetrafluoroborate salts **5a–e** (Scheme 5, Table 2). Electron-donating as well as electron-withdrawing substituents were tested on the aromatic ring without loss of efficiency. The lowest yield was observed with ortho-substituted **5d**, probably due to steric hindrance (Table 2, entry 4).



Scheme 5. Arylation of enol acetate **6** with diazonium salts **5a–e**.

Table 2. Scope of aryldiazonium tetrafluoroborate salts.

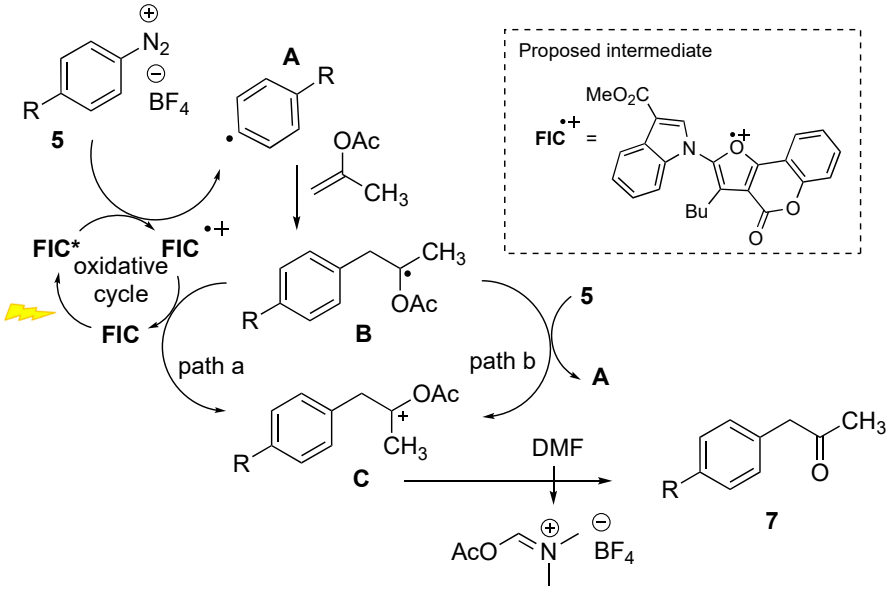
Entry	5	R	7 (%) [1]
1	**5a**	4-OMe	**7a** (80)
2	**5b**	4-NO_2	**7b** (77)
3	**5c**	H	**7c** (88)
4	**5d**	2-Br	**7d** (61)
5	**5e**	3-CN	**7e** (75)

[1] Isolated yield.

The proposed mechanism for the entire process, based on our investigation and on previous reports [22], is depicted in Scheme 6. Upon light irradiation, the excited photocatalyst (**FIC***) is oxidatively quenched by diazonium **5** to give an aryl radical intermediate **A** that can then be added regioselectively to the double bond of enol acetate **6**. At this stage, two pathways must be discussed. In path a, intermediate radical **B** can be oxidized by the photocatalyst (**FIC**$^{\bullet+}$) to regenerate **FIC** and give the intermediate carbocation **C**. According to previous literature [22], the latter can be deacetylated in the final step by DMF to generate the desired adduct **7**. In path a, **FIC** plays the role of a photocatalyst. In path b, radical intermediate **B** can react with starting diazonium **5** through a single electron transfer process to form intermediates **C** and **A**. In this last pathway, **FIC** plays the role of a photoinitiator only. It is important to note that in the absence of **FIC**, compound **7a** was still formed, but with a very low yield (Table 1, entry 3). This implies that the initiation step, i.e., the formation of the aryl radical **A**, may also be due to another mode of activation under irradiation [19]. However, the low yield obtained in this case argues in favor of path a in reactions where **FIC** is present, giving it the role of a real photocatalyst. Moreover, the fact that **FIC** can be recovered unchanged at the end of the reaction after purification on silica gel also supports this pathway.

2.2. Free Radical Polymerization (FRP) of Acrylates

Photopolymerization is now a highly efficient and versatile process that enables the rapid and sustainable fabrication of advanced materials, offering significant potential for applications in coatings, 3D printing, adhesives, and biomedical devices. This eco-friendly technique minimizes energy consumption and reduces waste, making it an ideal choice for greener industrial processes. Building on the high reactivity of **FIC** in organic synthesis, its potential application in photopolymerization processes has been thoroughly explored in mild LED irradiation conditions.



Scheme 6. Mechanistic hypothesis for the formation of **7**.

The photoinitiation abilities and the associated final acrylate function conversions of the newly developed photocatalyst (**FIC**) in the presence of either Iod as an additive (0.5%/1% *w*/*w*) or Iod and EDB (0.5%/1%/1% *w*/*w*/*w*) for the FRP of di(trimethylolpropane)tetraacrylate (**TA**) monomer were tested in thin films (25 µm, in laminate; Figure 1A) and thick samples (2.3 mm, in air; Figure 1B), using irradiation with a 365 nm LED. These experiments were also conducted under irradiation at 405 nm, but the results were more satisfactory by using a 365 nm LED. which is attributed to the higher absorption properties of the **FIC** photocatalyst at λ = 365 nm (Figure 2A).

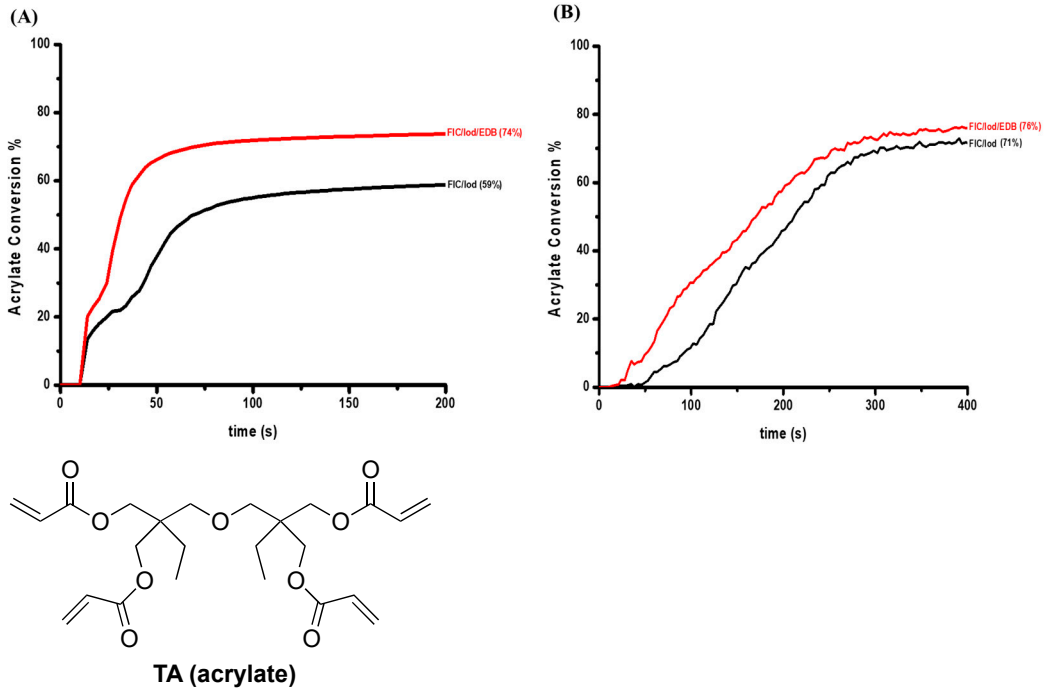


Figure 1. Photopolymerization profiles of **TA** (acrylate function conversion vs. irradiation time) upon exposure to a LED (λ = 365 nm) in the presence of **FIC**/Iod (0.5%/1% *w*/*w*) and **FIC**/Iod/EDB (0.5%/1%/1% *w*/*w*/*w*): (**A**) in laminate (thickness = 25 µm) and (**B**) in air (thickness = 2.3 mm). The irradiation starts at t = 10 s.

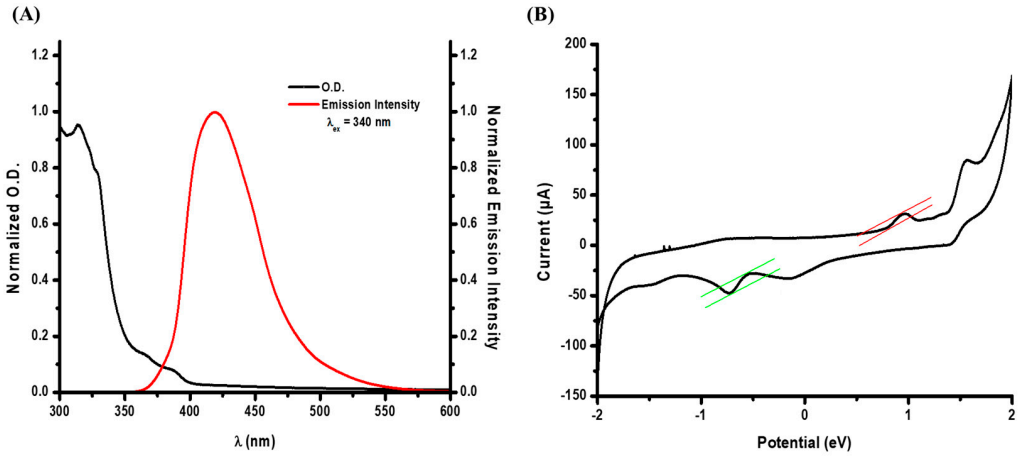


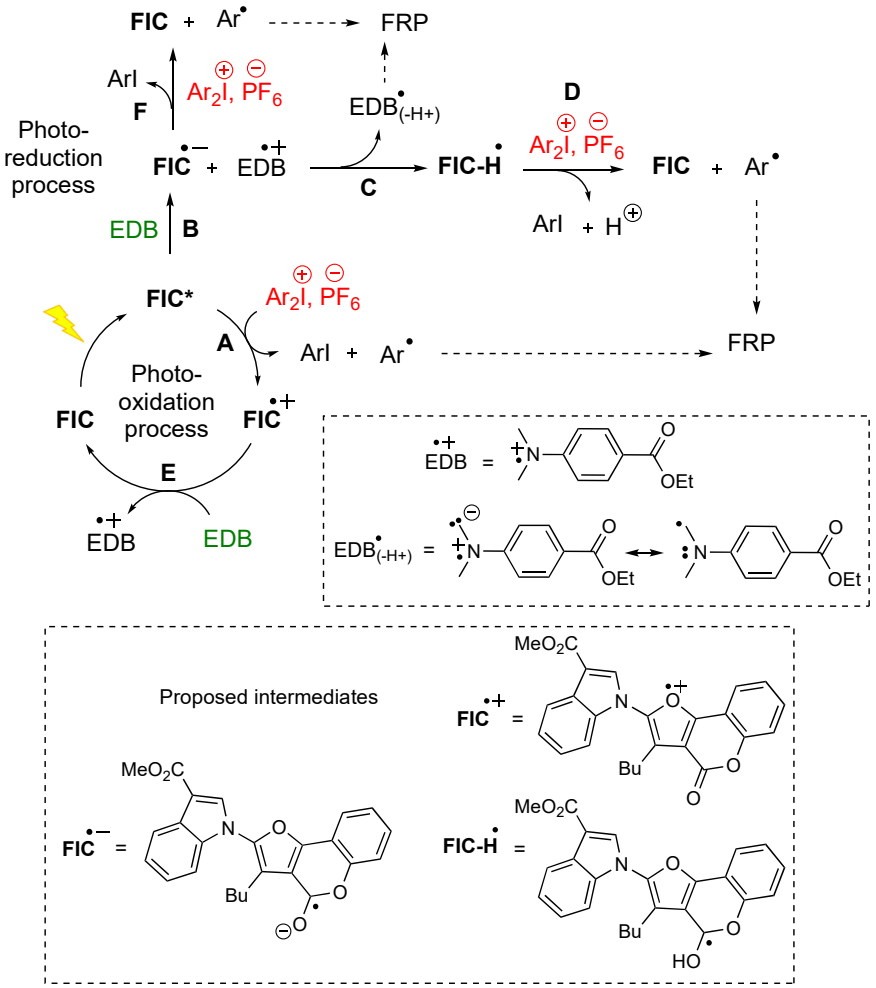
Figure 2. (**A**) UV-visible absorption and emission spectra of **FIC** in acetonitrile. (**B**) Cyclic voltammetry of **FIC** using tetrabutylammonium hexafluorophosphate dissolved in acetonitrile as the electrolyte.

It is noteworthy to mention that when investigated separately, the **FIC** photocatalyst, Iod, or EDB could not initiate the FRP of TA upon exposure to a 365 nm LED (Figure S1, see Supporting Information) where low final conversions of the acrylate functional group were observed (28%, 33% and 28%, respectively). Moreover, even though the combination of Iod/EDB (without **FIC**) would lead to a Charge Transfer Complex (CTC), the detected polymerization rate obtained was slow (only 40% of acrylate functions conversion within 200 s of irradiation; Figure S1), clearly showing the importance of the combination of the **FIC** photocatalyst with the aforementioned additives for an efficient process.

A good photopolymerization profile is attained by combining **FIC** with Iod in both thin and thick samples, where a relatively high % of acrylate functions conversion were achieved (59% and 71% respectively). This improvement is related to the formation of aryl radicals ($Ar^{\bullet}$) by a photo-oxidation process where an electron is transferred from the excited state of the photocatalyst **FIC*** to Iod (step A, Scheme 7). These radicals are considered to be the initiating species for the FRP. Furthermore, the addition of a third component (EDB) to the previous combination (**FIC**/Iod) leads to an increase in the % of acrylate conversion to 74% in thin samples and 76% in thick samples. For a tetrafunctional monomer, the conversions achieved in acrylate functions are remarkably high. This marked enhancement is ascribed to the generation of $EDB^{\bullet}{}_{(-H+)}$ radicals besides the formed aryl radicals, which are both responsible for initiating FRP. These $EDB^{\bullet}{}_{(-H+)}$ radicals are formed by a photo-reduction process where an electron is transferred from EDB to the excited state of the photocatalyst **FIC*** (step B, Scheme 7) followed by a proton abstraction (step C, Scheme 7). Additionally, $\mathbf{FIC}^{\bullet+}$ can react with EDB (step E, Scheme 7) or FIC-$H^{\bullet}$ with Iod (step D, Scheme 7) or $FIC^{\bullet-}$ with Iod (step F, Scheme 7), so that the photocatalyst **FIC** can be regenerated.

2.3. Photochemical Properties of FIC

To better understand the interaction between the newly investigated photocatalyst (**FIC**) and the additives (Iod and EDB), fluorescence quenching experiments, commonly used to show the involvement of bimolecular reactions from excited states [23], were carried out in acetonitrile. The concentration of Iod and EDB were increased cumulatively and each time a fluorescence spectrum was recorded.



Scheme 7. Mechanistic hypothesis for the FRP initiation.

Figure 3A,C show a prompt fluorescence quenching occurring for **FIC** with Iod and EDB, respectively, which evidently attest to the strong interaction of our photocatalyst (**FIC**) with both Iod and EDB (as shown in Scheme 7 (steps A and B)). Furthermore, the associated Stern–Volmer plots (Figure 3B,D) allow us to calculate the Stern–Volmer coefficients (K_{sv}) and the electron transfer quantum yields (Φ_{et}) [24], which are gathered in Table 3. High electron transfer quantum yields were obtained (0.8, and 0.95 for **FIC** with Iod and EDB, respectively) which also verifies the strong **FIC**/additives interaction and bimolecular electron transfer involving **FIC** and Iod, and **FIC** and EDB.

The singlet excited state energy E_{S1}, determined at 3.27 eV from the crossing point of the absorption and fluorescence spectra (Figure 2A), and the oxidation and reduction potentials (E_{ox} and E_{red}) determined by cyclic voltammetry (Figure 2B), allowed for the evaluation of the free energy change (ΔG) for the electron transfer reaction between **FIC** and the additives (Iod and EDB) (Table 3). Highly favorable ΔG are found in accordance with the strong **FIC**/Iod and strong **FIC**/EDB interactions observed in the fluorescence quenching experiments, supporting the proposed mechanism involving both the reduction of Iod and the oxidation of EDB (Scheme 7 (steps A and B)). Furthermore, the excited-state potentials **FIC***/**FIC**$^{\bullet-}$ (E^*_{red} = +2.64 V vs. SCE) and **FIC**$^{\bullet+}$/**FIC*** (E^*_{ox} = −2.41 V vs. SCE) calculated from these data using the very-well accepted method and equation in photochemistry [6,25] showed the powerful oxidative and reductive properties of **FIC** compared to already known metal- and organic-based photocatalysts (Scheme 1) [6,26]. To demonstrate these unique properties, other fluorescence bimolecular quenching experiments were conducted on **FIC** using substrates with high redox potentials (see Supplementary Materi-

als and Table S1). Prompt fluorescence quenching occurred for **FIC** using acetophenone (E_{red} = −2.11 V vs. SCE) in acetonitrile, which attests to the strong interaction of our photocatalyst (**FIC**) with this substrate (see Figure S2) and bimolecular electron transfer involving **FIC** and acetophenone. The associated Stern–Volmer plots allowed us to calculate the Stern–Volmer coefficients (K_{sv}) and the electron transfer quantum yields (Φ_{et} = 0.91). In addition, fluorescence quenching experiments conducted on **FIC** using anisole (E_{ox} = +1.75 V vs. SCE) and *o*-xylene (E_{ox} = +2.22 V vs. SCE) in cyclohexane (Figures S3 and S4) revealed the potential of our photocatalyst to also realize high-demanding oxidative processes. The high Stern–Volmer quenching verifies the favorable interaction between **FIC** and these substrates and bimolecular electron transfer involving **FIC** and anisole (Φ_{et} = 0.41), and **FIC** and *o*-xylene (Φ_{et} = 0.24).

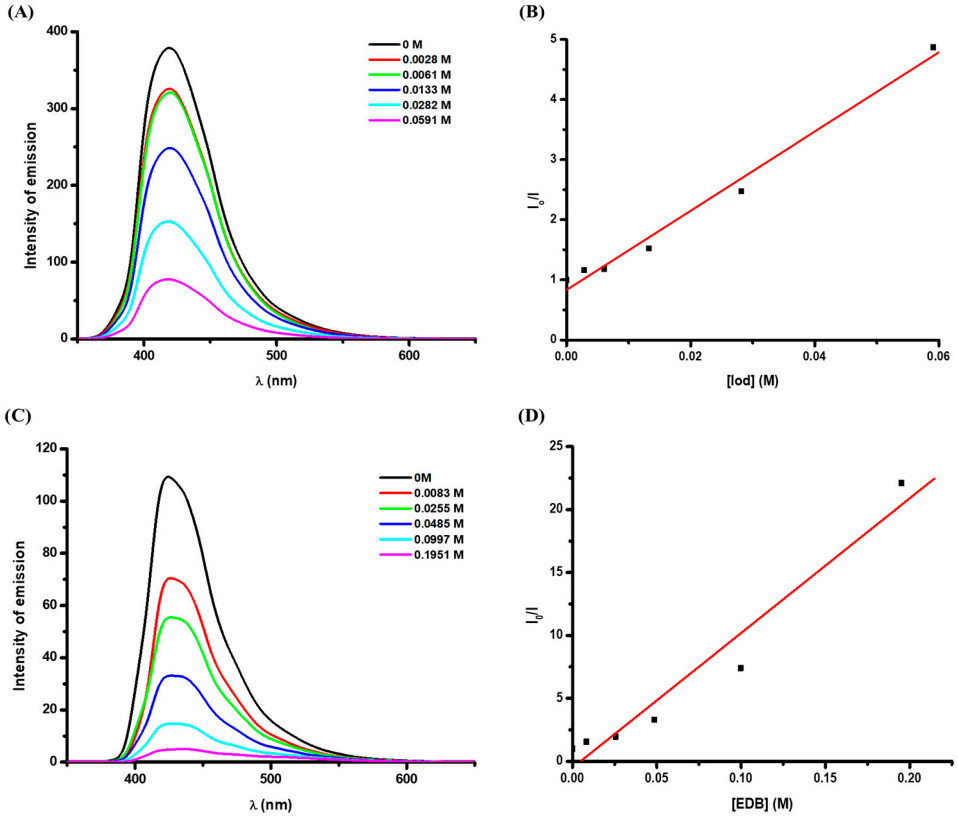


Figure 3. Fluorescence quenching study of **FIC**: (**A**) with Iod, and (**C**) with EDB in acetonitrile. Associated Stern–Volmer plot of **FIC**: (**B**) with Iod, and (**D**) with EDB.

Table 3. Parameters characterizing the chemical mechanisms associated with the **FIC**/Iod and **FIC**/EDB interactions in acetonitrile.

	E_{S1} (eV)	E_{ox} (V)	$\Delta G_{S1(FIC/Iod)}$ (eV) [a]	E_{red} (V)	$\Delta G_{S1(FIC/EDB)}$ (eV) [b]	$K_{sv\ (Iod)}$ (M^{-1}) [c]	$\Phi_{et\ (FIC/Iod)}$ [d]	$K_{sv\ (EDB)}$ (M^{-1}) [c]	$\Phi_{et\ (FIC/EDB)}$ [e]
FIC	3.27	0.86	−1.71	−0.63	−1.64	66	0.8	107	0.95

[a] Evaluated from $\Delta G_{S1\ (PI/Iod)} = E_{ox} - E_{red(Iod)} - E_{S1}$; $E_{red(Iod)}$ = −0.7 eV. [b] Evaluated from $\Delta G_{S1(PI/EDB)} = E_{ox(EDB)} - E_{red} - E_{S1}$; $E_{ox\ (EDB)}$ = 1 eV. [c] Stern–Volmer coefficient (K_{sv}): slope of the quenching curve ($I_0/I = 1 + Ksv[Iod]$). [d] Electron transfer quantum yield (Φ_{et}): obtained according to the following equation: $\Phi_{et} = k_{sv}[Iod]/(1 + k_{sv}[Iod])$ [24]. [e] Electron transfer quantum yield (Φ_{et}): obtained according to the following equation: $\Phi_{et} = k_{sv}[EDB]/(1 + k_{sv}[EDB])$ [24].

3. Materials and Methods

Synthesis of the studied Furane-Indole-Chromenone-based organic photocatalyst. The synthesis of methyl 1-(3-butyl-4-oxo-4H-furo[3,2-c]chromen-2-yl)-1H-indole-

3-carboxylate (**FIC**) was achieved in a two-step procedure using commercially available chemical compounds. Methyl indole-3-carboxylate (99%), 1-hexyne (97%) and 4-hydroxycoumarin were purchased from Sigma-Aldrich (St. Louis, MO, USA). The procedures are described in the Supplementary Materials.

Other chemical compounds. The chemical compounds used for the preparation of the resin mixtures were selected from the highest purity available and were used as received, and their chemical structures are represented. *Bis*-(4-*tert*-butylphenyl)iodonium hexafluorophosphate (Iod or SpeedCure 938) and ethyl-4-(dimethyl amino) benzoate were (Speedcure EDB) obtained from Lambson Ltd. (Wetherby, UK). The monomer used di(trimethylolpropane)tetraacrylate (TA) was obtained from Sartomer Europe (Paris, France). The storage stabilizer of the acrylate was not removed.

Photopolymerization kinetics (RT-FTIR). Detailed experimental conditions for each formulation have been cited in the captions of Figure 1 and Figure S1. The prepared formulations were stirred in the dark for 24 h. All polymerization experiments were performed using a 365 nm LED (incident light intensity at the sample surface I_0 = 15 mW·cm^{-2}) at room temperature, and the irradiation was initiated after t = 10 s. The weight of the system was calculated from the monomer content. The conversion of the acrylate function of TA was continuously followed by real-time Fourier transform infrared spectroscopy (JASCO FTIR 6600, Paris, France). For the thin samples (~25 µm in thickness), free radical polymerizations of TA were performed in laminate (the formulation is sandwiched between two polypropylene films to reduce the O_2 inhibition). The decrease of C=C double bond band was continuously followed from 1581 to 1662 cm^{-1}. For the thicker samples (~2.3 mm of thickness), the formulations were deposited on a polypropylene film inside a 2.3 mm mold in air. The evolution of the C=C band was continuously followed from 6117 to 6221 cm^{-1}. The final acrylate function conversion of TA was obtained using the following equation:

$$\mathrm{FC}(\%) = \frac{\mathrm{Ao} - \mathrm{At}}{\mathrm{Ao}} \times 100$$

where FC is the final function conversion, A_0 is the proportion of the peak area at 0 s, and A_t is the portion of the peak area at t s. The procedure has been already described by our group in reference [24].

Steady state fluorescence. The investigation of the fluorescence properties of **FIC** in acetonitrile was done using a JASCO FP-6200 spectrofluorimeter (Paris, France). Fluorescence quenching experiments on **FIC** using the cumulative addition of Iod or EDB (concentrations mentioned in Figure 2) were done by means of the JASCO FP-6200 spectrofluorimeter. The concentration of **FIC** used throughout the experiments was 5×10^{-5} M. The calculation of the Stern–Volmer coefficients (K_{sv}) and the electron transfer quantum yields (Φ_{et}) was done according to the equations mentioned in Table 3.

UV-Visible absorption experiment. The UV-visible absorption properties of **FIC** were examined for the calculation of the singlet excited state energy E_{S1} in acetonitrile using a JASCO V730 spectrometer (Paris, France). The concentration of **FIC** used throughout this experiment was 4×10^{-5} M.

Oxidation and reduction potentials. Oxidation and reduction potentials for **FIC** (E_{ox} and E_{red}) were measured using cyclic voltammetry, with tetrabutylammonium hexafluorophosphate dissolved in acetonitrile as the electrolyte (potentials vs. Saturated Calomel Electrode—SCE). The free energy change (ΔG_{et}) for the electron transfer reactions of **FIC** with both Iod and EDB were calculated using Equation (1), [12] where E_{ox}, E_{red}, E*, and C stand for the oxidation potential of the electron donor, the reduction potential of the electron acceptor, the considered excited state energy level and the coulombic term for the initially formed ion pair, respectively. Here, the reduction potential of Iod is E_{red}(Iod) = −0.7 V, the

oxidation potential of EDB is E_{ox}(EDB) = 1 V, and C was neglected, as is usually done for polar solvents [12].

$$\Delta G_{et} = E_{ox} - E_{red} - E^* + C \quad (1)$$

4. Conclusions

This study highlighted the photochemical properties of a member of a new family of light sensitive organic molecule. Furane-indole-chromenone-based organic derivative (**FIC**), which can be synthetized in a half-gram scale using a simple two-step procedure, has demonstrated its ability to behave as a photocatalyst in the α-arylation of enol acetate upon LED irradiation at 405 nm, and as a photoinitiator/photocatalyst in the free radical polymerization of an acrylate group in the presence of Iod as an additive or in the presence of both Iod and EDB under LED irradiation at 365 nm. The use of classical techniques such as fluorescence quenching experiments, UV-visible absorption and fluorescence spectroscopy, and cyclic voltammetry analysis enabled us to understand the mechanisms involved, and revealed the wide redox window (3.27 eV) and the high excited-state potentials (from −2.41 to +2.64 V) offered by this new photocatalyst, which can be engaged in both oxidative and reductive quenching processes. Future developments, related to the tuning of the properties of furane-indole-chromenone-based architecture that can be activated at longer wavelengths in photocatalyzed reactions, and free radical polymerization, will be proposed in upcoming studies. The use of more challenging substrates such as halogeno-arenes instead of diazonium or iodonium salts as a radical precursor will be reported soon.

Supplementary Materials: The following supporting information can be downloaded at: https://www.mdpi.com/article/10.3390/molecules30020265/s1, Figure S1: Photopolymerization profiles of TA; Figures S2, S3 and S4: Fluorescence quenchings for **FIC**. Table S1: parameters characterizing the **FIC**/electron donor or acceptor systems. Experimental procedures, product characterization data. References [27–34] are cited in the Supplementary Materials.

Author Contributions: Conceptualization, J.L. and L.F.; validation, A.G.-G., A.N., J.L. and L.F.; investigation, A.G.-G. and A.N.; writing—original draft preparation, L.F.; writing—review and editing, A.G.-G., A.N., J.L., E.B. and S.G.; visualization, A.G.-G. and A.N.; supervision, J.T., T.H., J.L. and L.F.; project administration, J.L. and L.F. All authors have read and agreed to the published version of the manuscript.

Funding: This research received no external funding.

Institutional Review Board Statement: Not applicable.

Informed Consent Statement: Not applicable.

Data Availability Statement: The data underlying this study are available in the published article and its Supporting Information.

Acknowledgments: The authors acknowledge Aix Marseille University for funding Aurélien Galibert-Guijarro's thesis.

Conflicts of Interest: The authors declare no conflicts of interest.

References

1. Gadde, K.; De Vos, D.; Maes, B.U.W. Basic Concepts and Activation Modes in Visible-Light Photocatalyzed Organic Synthesis. *Synthesis* **2023**, *55*, 164–192. [CrossRef]
2. De Vos, D.; Gadde, K.; Maes, B.U.W. Emerging Activation Modes and Techniques in Visible-Light-Photocatalyzed Organic Synthesis. *Synthesis* **2023**, *55*, 193–231. [CrossRef]
3. Romero, N.A.; Nicewicz, D.A. Organic Photoredox Catalysis. *Chem. Rev.* **2016**, *116*, 10075–10166. [CrossRef] [PubMed]
4. Lee, Y.; Kwon, M.S. Emerging Organic Photoredox Catalysts for Organic Transformations. *Eur. J. Org. Chem.* **2020**, *2020*, 6028–6043. [CrossRef]

5. Bell, J.D.; Murphy, J.A. Recent Advances in Visible Light-Activated Radical Coupling Reactions Triggered by (i) Ruthenium, (Ii) Iridium and (Iii) Organic Photoredox Agents. *Chem. Soc. Rev.* **2021**, *50*, 9540–9685. [CrossRef]
6. Wu, Y.; Kim, D.; Teets, T.S. Photophysical Properties and Redox Potentials of Photosensitizers for Organic Photoredox Transformations. *Synlett* **2022**, *33*, 1154–1179.
7. Bobo, M.V.; Kuchta, J.J.; Vannucci, A.K. Recent Advancements in the Development of Molecular Organic Photocatalysts. *Org. Biomol. Chem.* **2021**, *19*, 4816–4834. [CrossRef] [PubMed]
8. Speckmeier, E.; Fischer, T.G.; Zeitler, K. A Toolbox Approach To Construct Broadly Applicable Metal-Free Catalysts for Photoredox Chemistry: Deliberate Tuning of Redox Potentials and Importance of Halogens in Donor–Acceptor Cyanoarenes. *J. Am. Chem. Soc.* **2018**, *140*, 15353–15365. [CrossRef] [PubMed]
9. Zivic, N.; Kuroishi, P.K.; Dumur, F.; Gigmes, D.; Dove, A.P.; Sardon, H. Recent advances and challenges in the design of organic photoacid and photobase generators for polymerizations. *Angew. Chem. Int. Ed.* **2019**, *58*, 10410–10422. [CrossRef] [PubMed]
10. Chatani, S.; Kloxin, C.J.; Bowman, C.N. The power of light in polymer science: Photochemical processes to manipulate polymer formation, structure, and properties. *Polym. Chem.* **2014**, *5*, 2187–2201. [CrossRef]
11. Crivello, J.V.; Reichmanis, E. Photopolymer materials and processes for advanced technologies. *Chem. Mater.* **2014**, *26*, 533–548. [CrossRef]
12. Gibson, I.; Rosen, D.W.; Stucker, B. Photopolymerization processes. In *Additive Manufacturing Technologies: Rapid Prototyping to Direct Digital Manufacturing*, 1st ed.; Springer: New York, NY, USA, 2010; pp. 78–119.
13. Yoshino, F.; Yoshida, A. Effects of blue-light irradiation during dental treatment. *Jpn. Dent. Sci. Rev.* **2018**, *54*, 160–168. [CrossRef]
14. Yang, H.; Li, G.; Stansbury, J.W.; Zhu, X.; Wang, X.; Nie, J. Smart antibacterial surface made by photopolymerization. *ACS Appl. Mater. Interfaces* **2016**, *8*, 28047–28054. [CrossRef] [PubMed]
15. Geisler, E.; Lecompère, M.; Soppera, O. 3D printing of optical materials by processes based on photopolymerization: Materials, technologies, and recent advances. *Photonics Res.* **2022**, *10*, 1344–1360. [CrossRef]
16. Jandt, K.D.; Mills, R.W.; Blackwell, G.B.; Ashworth, S.H. Depth of cure and compressive strength of dental composites cured with blue light emitting diodes (LEDs). *Dent. Mater.* **2000**, *16*, 41–47. [CrossRef]
17. Dreyer, C.; Mildner, F. Application of LEDs for UV-curing. In *III-Nitride Ultraviolet Emitters: Technology and Applications*, 1st ed.; Springer: Cham, Switzerland, 2016; pp. 415–434.
18. Galibert-Guijarro, A.; Mouysset, D.; Mimoun, L.; Bertrand, M.P.; Feray, L. Ynamides in Radical Reactions: A Route to Original Persubstituted 2-Aminofurans. *J. Org. Chem.* **2023**, *88*, 2464–2473. [CrossRef] [PubMed]
19. Galli, C. Radical Reactions of Arenediazonium Ions: An Easy Entry into the Chemistry of the Aryl Radical. *Chem. Rev.* **1988**, *88*, 765–792. [CrossRef]
20. De Souza, E.L.S.; Oliveira, C.C. Selective Radical Transformations with Aryldiazonium Salts. *Eur. J. Org. Chem.* **2023**, *26*, e202300073. [CrossRef]
21. Schroll, P.; Hari, D.P.; König, B. Photocatalytic Arylation of Alkenes, Alkynes and Enones with Diazonium Salts. *ChemistryOpen* **2012**, *1*, 130–133. [CrossRef]
22. Hering, T.; Hari, D.P.; König, B. Visible-Light-Mediated α-Arylation of Enol Acetates Using Aryl Diazonium Salts. *J. Org. Chem.* **2012**, *77*, 10347–10352. [CrossRef]
23. Tomin, V.I. Studying reactions that proceed from highest excited states of molecules using fluorescence quenching. *Opt. Spectrosc.* **2008**, *105*, 496–510. [CrossRef]
24. Noon, D.; Hammoud, F.; Graff, B.; Hamieh, T.; Toufaily, J.; Morlet-Savary, F.; Schmitt, M.; Bui, T.-T.; Rico, A.; Goubard, F.; et al. Photoinitiation Mechanisms of Novel Phenothiazine-Based Oxime and Oxime Esters Acting as Visible Light Sensitive Type I and Multicomponent Photoinitiators. *Adv. Mater. Technol.* **2023**, *8*, 2300205. [CrossRef]
25. Fehér, P.P.; Madarász, Á.; Stirling, A. Prediction of Redox Power for Photocatalysts: Synergistic Combination of DFT and Machine Learning. *J. Chem. Theory Comput.* **2023**, *19*, 4125–4135. [CrossRef]
26. Mateos, J.; Rigodanza, F.; Vega-Peñaloza, A.; Sartorel, A.; Natali, M.; Bortolato, T.; Pelosi, G.; Companyó, X.; Bonchio, M.; Dell'Amico, L. Naphthochromenones: Organic Bimodal Photocatalysts Engaging in Both Oxidative and Reductive Quenching Processes. *Angew. Chem. Int. Ed.* **2020**, *59*, 1302–1312. [CrossRef] [PubMed]
27. Roe, A. Preparation of aromatic fluorine compounds from diazonium fluoborates. The Schiemann reaction. *Org. React.* **1949**, *5*, 193.
28. Tang, Z.Y.; Zhang, Y.; Wang, T.; Wang, W. Rhodium (I)-catalyzed synthesis of aryltriethoxysilanes from arenediazonium tosylate salts with triethoxysilane. *Synlett* **2010**, *5*, 804–808.
29. Xu, Y.; Alcock, N.W.; Clarkson, G.J.; Docherty, G.; Woodward, G.; Wills, M. Asymmetric hydrogenation of ketones using a ruthenium (II) catalyst containing binol-derived monodonor phosphorus-donor ligands. *Org. Lett.* **2004**, *6*, 4105–4107. [CrossRef] [PubMed]
30. Li, L.; Cai, P.; Guo, Q.; Xue, S.J. Et_2Zn-mediated rearrangement of bromohydrins. *Org. Chem.* **2008**, *73*, 3516–3522. [CrossRef]

31. Molinaro, C.; Mowat, J.; Gosselin, F.; O'Shea, P.D.; Marcoux, J.-F.; Angelaud, R.; Davies, I.W.J. A practical synthesis of α-aryl methyl ketones via a transition-metal-free meerwein arylation. *Org. Chem.* **2007**, *72*, 1856–1858. [CrossRef] [PubMed]
32. Yuan, L.Z.; Zhao, G.; Hamze, A.; Alami, M.; Provot, O. Chlorotrimethylsilane and Sodium Iodide: A Useful Combination for the Regioselective Deoxygenation of Arylalkyl-α-Diketones. *Adv. Synth. Catal.* **2017**, *359*, 2682–2691. [CrossRef]
33. Hisano, N.; Kamei, Y.; Kansaku, Y.; Yamanaka, M.; Mori, K. Construction of 1, 3-Dithio-substituted Tetralins by [1, 5]-alkylthio group transfer mediated skeletal rearrangement. *Org. Lett.* **2018**, *20*, 4223–4226. [CrossRef] [PubMed]
34. Wang, L.; Shen, J.; Yang, S.; Liu, W.; Chen, Q.; He, M. C–H arylation reactions through aniline activation catalysed by a PANI-gC_3N_4-TiO_2 composite under visible light in aqueous medium. *Green Chem.* **2018**, *20*, 1290–1296. [CrossRef]

Disclaimer/Publisher's Note: The statements, opinions and data contained in all publications are solely those of the individual author(s) and contributor(s) and not of MDPI and/or the editor(s). MDPI and/or the editor(s) disclaim responsibility for any injury to people or property resulting from any ideas, methods, instructions or products referred to in the content.